ISSN: 1692-7257 - Volume 2 – Number 48 - 2026

RCTA
Revista Colombiana de Tecnologías de Avanzada
UNIPAMPLONA

Site-Specific Modeling of Continuous Electromagnetic Field Exposure in Bogotá

Modelación específica por sitio de la exposición continua a campos electromagnéticos en Bogotá

PhD. Osnamir Elias Bru-Cordero[1], **PhD. Juan Guillermo Popayán Hernández**[1], **PhD. Cristian David Correa Álvarez**[2]

[1] **Universidad Nacional de Colombia,** Sede De La Paz, Dirección Académica, La Paz, Cesar, Colombia.
[2] **Universidad Nacional de Colombia,** Sede Manizales, Departamento de Matemáticas y Estadística, Manizales, Colombia.

Correspondence: oebruc@unal.edu.co

Received: april 17, 2026. **Revised:** june 25, 2026. **Accepted:** july 24, 2026. **Published:** july 27, 2026.

How to cite: O. E. Bru-Cordero, J. G. Popayán Hernández, and C. D. Correa Álvarez, "Site-Specific Modeling of Continuous Electromagnetic Field Exposure in Bogotá", *Revista Colombiana de Tecnologías de Avanzada (RCTA)*, vol. 2, no. 48, pp. 155–165, jul. 2026, doi: 10.24054/rcta.v2i48.4411

This work is licensed under a
Creative Commons Attribution-NonCommercial 4.0 International License.

Abstract: This study develops and validates a reproducible, site-sensitive workflow for analyzing continuous electromagnetic field monitoring data published as open data by the National Spectrum Agency (ANE) of Colombia. The Bogotá subset contains 481,148 broadband electric field measurements averaged over six-minute intervals, collected by nine fixed probes between November 2, 2023, and June 30, 2024. After harmonizing timestamps and applying a completeness filter, 2,009 probe-day records were analyzed. To account for the longitudinal structure of the dataset, two ordinary least squares log-linear specifications with HC3 robust inference were compared with a random-intercept mixed-effects model, and an additional model was estimated for the daily 95th percentile. The temporal-only model explained little variation in mean daily exposure (adjusted R^2 = 0.007), whereas the model with probe fixed effects captured most of the variability (adjusted R^2 = 0.964). The mixed-effects model led to the same interpretation (marginal R^2 = 0.016; conditional R^2 = 0.964), while the p95 model retained a strongly site-dependent structure (adjusted R^2 = 0.951). Regression diagnostics indicated non-normality, heteroscedasticity, and positive residual autocorrelation, but no high-leverage observations or influential observation capable of explaining the high model fit were identified. The maximum six-minute field observed was 0.21011 V/m, below 1% of the public contextual reference value of 28 V/m. The differential contribution of this study is not to make a general claim that site conditions matter, but rather to validate this structure specifically for Bogotá through an auditable open-data workflow that reports complete coefficients, diagnostics, and robustness in the upper tail.

Keywords: electromagnetic field monitoring; Bogotá; open data; fixed-effects modeling; mixed-effects models; regression diagnostics; telecommunications infrastructure.

Resumen: Este estudio desarrolla y valida un flujo de trabajo reproducible y sensible al sitio para analizar datos continuos de monitoreo de campos electromagnéticos publicados como datos abiertos por la Agencia Nacional del Espectro (ANE) de Colombia. El subconjunto de Bogotá contiene 481.148 mediciones de campo eléctrico de banda ancha promediadas cada seis minutos, recolectadas por nueve sondas fijas entre el 2 de noviembre de 2023 y el 30 de junio de 2024. Tras armonizar las marcas de tiempo y aplicar un filtro de completitud, se analizaron 2.009 registros sonda-día. Para atender la estructura longitudinal del archivo, se compararon dos especificaciones log-lineales de mínimos cuadrados ordinarios con inferencia robusta HC3 con un modelo mixto de intercepto aleatorio, y además se estimó un modelo complementario para el percentil 95 diario. El modelo solo temporal explicó poca variación en la exposición media diaria (R^2 ajustado = 0,007), mientras que el modelo con efectos fijos por sonda capturó la mayor parte de la variabilidad (R^2 ajustado = 0,964). El modelo mixto condujo a la misma interpretación (R^2 marginal = 0,016; R^2 condicional = 0,964), y el modelo p95 conservó una estructura fuertemente dependiente del sitio (R^2 ajustado = 0,951). Los diagnósticos de regresión mostraron no normalidad, heterocedasticidad y autocorrelación residual positiva, pero no observaciones con leverage alto ni una observación influyente capaz de explicar el alto ajuste. El campo máximo observado en seis minutos fue 0,21011 V/m, por debajo del 1% de la referencia contextual pública de 28 V/m. La contribución diferencial del estudio no es afirmar de forma general que las condiciones del sitio importan, sino validar esta estructura de manera específica para Bogotá mediante un flujo auditable de datos abiertos que reporta coeficientes completos, diagnósticos y robustez en la cola superior.

Palabras clave: monitoreo de campos electromagnéticos; Bogotá; datos abiertos; modelación con efectos fijos; modelos mixtos; diagnósticos de regresión; infraestructura de telecomunicaciones.

1. INTRODUCTION

Electromagnetic field (EMF) exposure associated with wireless communication systems remains a technical and regulatory issue because telecommunications infrastructure continues to expand while spectrum authorities need transparent evidence on public radiofrequency conditions. The World Health Organization frames EMF exposure as both an engineering and communication challenge, and the long-duration monitoring approach formalized in ITU-T Recommendation K.83 was created to support that need [1]–[3].

In Colombia, this monitoring logic is reflected in the regulatory framework for non-ionizing radiation and in the open-data publication strategy of the Agencia Nacional del Espectro (ANE), which releases continuous records from its EMF monitoring system [4], [5]. The engineering implication is that exposure assessment is no longer limited to isolated field campaigns; it has become part of infrastructure oversight, spectrum governance, and technical accountability.

International literature shows that continuous monitoring has matured into a practical tool for engineering interpretation and public communication. Reviews on EMF monitoring concepts, measurement instruments, and microenvironmental exposure patterns have documented the value of broadband observations for characterizing low-level public exposure and for comparing monitoring strategies across contexts [7]–[9]. Continuous observatory systems in Greece and other countries further show that long-duration fixed-site measurements can identify stable exposure patterns, seasonal modulation, and persistent site differences while remaining well below public reference levels [10]–[12].

A second branch of the literature emphasizes that radiofrequency exposure patterns are shaped by local site conditions rather than by time alone. Surveys around base stations, urban wireless systems, and residential areas have repeatedly found that measured field levels depend on transmitter geometry, surrounding urban form, network density, and the composition of active services [13]–[15]. Modeling-oriented studies have extended this insight through geospatial, surrogate, and spatio-temporal approaches, demonstrating that exposure data become more useful for engineering decisions when they are converted into interpretable statistical models rather than treated only as isolated measurements [16]–[20]. More recent work on long-term monitoring, small cells, and 5G environments confirms that temporal variation exists, but that the strongest structure often remains site-dependent [12], [23]–[25].

The scientific gap addressed here is therefore more specific than the general observation that sites differ. For Latin American open-data archives, there are still few reproducible studies that audit the semantics of public monitoring variables, separate site baselines from calendar effects within one metropolitan environment, report full model outputs, and test whether the same conclusion holds for both routine exposure and upper-tail indicators such as the 95th percentile. This gap matters because a national open-data release mixes cities, probes, and operating histories; without a site-aware and diagnostic-rich workflow, public monitoring data can be summarized but not fully interpreted for local engineering decisions.

Accordingly, this paper develops a Bogotá-specific statistical analysis of the ANE continuous monitoring archive. The objectives are to characterize the Bogotá subset after transparent preprocessing, compare a temporal-only specification with a probe-adjusted fixed-effects model for daily mean electric-field intensity, evaluate regression diagnostics and panel-aware robustness through a mixed model, and test whether a complementary p95 model supports the same interpretation. The differential contribution is an auditable workflow that converts a Colombian open monitoring archive into interpretable site-level evidence for benchmarking, anomaly screening, and public technical communication.

2. MATERIALS AND METHODS

2.1. Open dataset and Bogotá analytical scope

The raw data came from the open government repository "Mediciones de exposición a campos electromagnéticos" maintained by the ANE [5]. The national CSV release contains the fields Ubicacion_Sonda, Ciudad_Departamento, Fecha_Medicion, Nivel_Exposicion, Limite_Restrictivo, Porcentaje_Exposicion, and Punto_Georreferenciado.

In its released form, the file comprised 1,286,346 six-minute measurements obtained from 26 probes distributed across 12 city–department labels. The present study restricted the analysis to the Bogotá subset because it provides the largest number of probes within a common metropolitan setting and is therefore better suited to evaluating site-specific monitoring behavior without conflating it with intercity differences.

After filtering by probe identifier, the Bogotá subset contained 481,148 six-minute broadband electric-field records collected by nine fixed probes between 2 November 2023 and 30 June 2024. The analytical variable of interest was Nivel_Exposicion, defined in the ANE technical documentation as RMS electric-field intensity in V/m measured by broadband isotropic monitoring equipment under the long-duration logic of ITU-T K.83 [3], [5].

The current CSV release includes Limite_Restrictivo and Porcentaje_Exposicion, but those variables were not used as inferential modeling targets because the released file encodes a constant restrictive value of 2, whereas the archived support document describes a contextual public reference of 28 V/m for the published dataset [4], [5]. To avoid propagating undocumented transformations, all inferential analysis was based on the directly measured field intensity in V/m. Percentages relative to 28 V/m were retained only for contextual descriptive reporting.

2.2. Preprocessing and descriptive indicators

Timestamp preprocessing converted Fecha_Medicion into valid calendar datetimes using the format "Y b d I:M:S p", after which the data were aggregated by probe and calendar day. For each probe-day, the workflow computed the number of valid six-minute records, the daily mean field, daily median, daily 95th percentile, and daily maximum. Because the monitoring logic is based on six-minute averaging, a nominal full day contains 240 observations. To ensure comparable daily windows, the analysis retained only probe-days with at least 200 valid records.

The resulting analytical sample contained 2,009 retained probe-day records, with an average of 239.1 six-minute measurements per retained day. Month and day of the week were derived from the calendar date. Unlike the previous version of the manuscript, the daily p95 was not left only as a descriptive indicator: it was retained descriptively and was also modeled as an upper-tail robustness target to verify whether the mean-based interpretation held for high-end routine exposure.

2.3. Statistical models, longitudinal justification, and diagnostics

Two complementary log-linear models were estimated for daily mean electric-field intensity. Model A evaluated calendar effects only, whereas Model B added probe fixed effects to capture persistent site heterogeneity. The logarithmic transformation was used because daily field values were positive, right-skewed, and easier to interpret multiplicatively after exponentiating coefficients.

$$\log(MeanE\_pd + 10^{-6}) = \beta 0 + \gamma m + \delta w + \varepsilon pd. \quad (1)$$
$$\log(MeanE\_pd + 10^{-6}) = \beta 0 + \alpha p + \gamma m + \delta w + \varepsilon pd. \quad (2)$$

In Equations (1) and (2), p denotes the probe, d the calendar day, m the month, and w the day of the week. The term αp represents the probe-specific fixed effect, γm the monthly effect, δw the weekday effect, and εpd the unexplained component. Ordinary least squares was retained as the primary estimator because the purpose was to estimate interpretable fixed site baselines within the observed monitoring network rather than to predict unobserved probes. This fixed-effects formulation is a standard panel-data strategy for removing time-invariant site heterogeneity [26], [27].

To address the longitudinal nature of the data, Model B was not treated as the only evidence. A random-intercept mixed model, log(MeanEpd + 10^-6) = β0 + up + γm + δw + εpd, with up representing a probe-level random intercept, was estimated as a panel-aware robustness check. The mixed model tests whether the same site-dominant interpretation appears when the probe structure is represented as a random effect rather than as a fixed set of site indicators [26].

The p95 issue raised during review was addressed by estimating a third model with the same predictors as Model B but replacing the response with log(p95Epd + 10^-6). This model does not replace the daily mean specification; it verifies whether the upper tail of routine exposure follows the same site and calendar structure.

$$\log(p95E\_pd + 10^{-6}) = \beta 0 + \alpha p + \gamma m + \delta w + \varepsilon pd. \quad (3)$$

Coefficient inference for the OLS models used HC3 heteroskedasticity-consistent covariance matrices. Complete coefficient tables report estimates, robust standard errors, 95% confidence intervals, p-values, and exponentiated effects. Model adequacy was evaluated through residual normality tests, heteroskedasticity tests, residual-versus-fitted plots, Q-Q plots, studentized residuals, leverage, Cook's distance, pooled Durbin-Watson values, and probe-level lag-1 residual autocorrelation. These diagnostics are used to qualify the strength of inference rather than to hide model limitations [28].

2.4. Reproducibility framework

The revised workflow was scripted in R [22] using readr, dplyr, lubridate, ggplot2, sandwich, lmtest, broom, tidyr, forcats, and nlme. The updated script automates data import, timestamp parsing, Bogotá filtering, probe-day aggregation, completeness filtering, descriptive summaries, model estimation, HC3 inference, full coefficient export, p95 modeling, mixed-effects robustness, diagnostic tables, diagnostic figures, and session-information export. This reproducible structure is important not only for transparency but also because the open dataset requires semantic auditing before derived limit-related variables are interpreted.

3. RESULTS AND DISCUSSION

3.1. Descriptive characterization of the Bogotá monitoring archive

Table 1 summarizes the Bogotá analytical subset obtained after the full preprocessing sequence. The city-specific archive retained 481,148 six-minute broadband records and 2,009 near-complete probe-day observations from nine monitoring probes. The observation window extended from 2 November 2023 to 30 June 2024, and the average retained probe-day contained 239.1 valid six-minute measurements. The overall mean of the daily mean field was 0.02679 V/m, whereas the overall mean of the daily p95 was 0.03791 V/m.

The maximum six-minute field observed in the Bogotá subset was 0.21011 V/m, which remains below 1% of the contextual 28 V/m public reference described in the archived ANE support document [4], [5]. This magnitude is consistent with continuous monitoring studies that report low public exposure levels even in dense urban environments [10], [15], [21].

Table 1. Summary of the Bogotá analytical subset.

Metric	Value
Raw Bogotá six-minute records	481,148
Retained probe-day records	2,009
Distinct Bogotá probes	9
Observation period	2023-11-02 to 2024-06-30
Mean six-minute records per retained day	239.1
Overall mean of daily mean E (V/m)	0.02679
Overall median of daily mean E (V/m)	0.01060
Overall mean of daily p95 E (V/m)	0.03791
Maximum observed six-minute field (V/m)	0.21011
Maximum daily mean as % of 28 V/m	0.49

RCTA
Revista Colombiana de Tecnologías de Avanzada
UNIPAMPLONA

Maximum daily p95 as % of 28 V/m	0.60

Source: own elaboration from ANE open data. Values relative to 28 V/m are contextual descriptors, not inferential targets.

The strongest descriptive feature of the Bogotá subset is between-probe heterogeneity. Table 2 and Fig. 1 show that Bogota_AEROCIVIL presented the highest mean daily field (0.12759 V/m), followed by Bogota_ANE_2 (0.04944 V/m), whereas Bogota_TES_1 averaged only 0.00243 V/m. This represents a more than fifty-fold difference between the highest and lowest average probe.

***Table 2:** Bogotá probe ranking by mean daily electric-field level.*

Probe	Days	Mean daily E	Mean daily p95	Maximum observed E	Mean % of 28 V/m
Bogota_AEROCIVIL	242	0.12759	0.15116	0.21011	0.456
Bogota_ANE_2	199	0.04944	0.08642	0.15932	0.177
Bogota_MINTIC	242	0.01679	0.03176	0.12665	0.06
Bogota_BATALLON_BARAYA	207	0.01144	0.01746	0.02435	0.041
Bogota_CAN_CGFM	209	0.01115	0.01699	0.02819	0.04
Bogota_AEROPUERTO_GUAYMARAL	242	0.0091	0.01757	0.02941	0.032
Bogota_ANE	234	0.00386	0.00734	0.03495	0.014
Bogota_BATALLON_USME	208	0.00332	0.00398	0.00749	0.012
Bogota_TES_1	226	0.00243	0.00328	0.00629	0.009

***Source:** own elaboration. Mean percentages are relative to 28 V/m.*

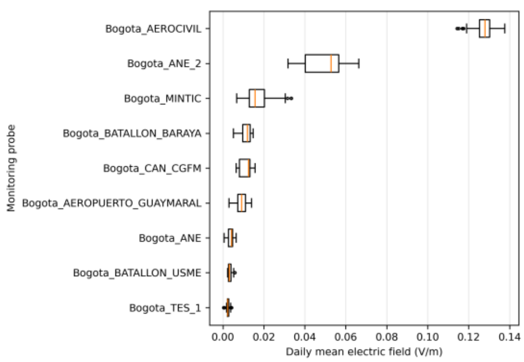

***Fig. 1.** Distribution of daily mean electric field across Bogotá monitoring probes. **Source:** own elaboration.*

The raw temporal profiles are informative but must be interpreted cautiously because unequal probe availability can mix temporal effects with site composition. Monthly averages show modest variation in both daily mean and p95 values, while weekday averages show lower Saturday and Sunday levels than Tuesday through Friday. These patterns motivated the adjusted models reported below.

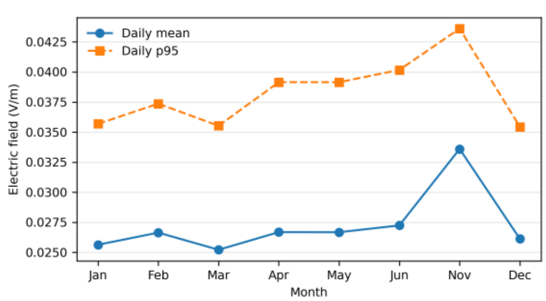

***Fig. 2.** Monthly averages of daily mean and daily p95 electric-field values in Bogotá. **Source:** own elaboration.*

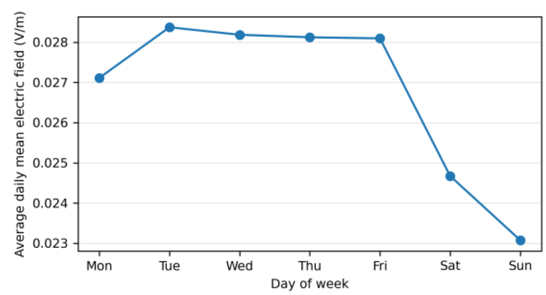

***Fig. 3.** Weekday averages of daily mean electric field in Bogotá. **Source:** own elaboration.*

3.2. Temporal-only versus probe-adjusted modeling

Table 3 compares the daily mean models and the complementary p95 model. Model A, which included only month and day-of-week terms, explained almost none of the variability in daily mean exposure (adjusted $R^2 = 0.007$). Model B, which added probe fixed effects, changed the result substantially: the adjusted R^2 rose to 0.964 and the residual standard error fell from 1.270 to 0.242 on the log scale. The contrast between the two specifications is the central empirical result of the article. In Bogotá, broad calendar structure alone is not sufficient to characterize daily mean field intensity; most explainable variability is tied to the monitoring site itself.

Table 3: *Comparison of mean-based and p95 log-linear models.*

Model	Target	Adjusted R^2	AIC (R-style)	Residual SE
A: month + day of week	Daily mean E	0.007	6678.6	1.270
B: month + day of week + probe fixed effects	Daily mean E	0.964	25.9	0.242
C: p95 upper-tail model (month + day + probe)	Daily p95 E	0.951	640.6	0.282

AIC values follow the R lm convention used by the updated reproducibility script. ***Source:*** *own elaboration.*

Tables 4A and 4B provide the complete coefficient output requested during review. Coefficients are reported on the log scale. Exp(beta) gives the multiplicative factor relative to the reference category. In Model B, the reference profile is Bogota_AEROCIVIL in January on Monday.

Table 4A: *Complete HC3 coefficient table for Model A: log daily mean E ~ month + day of week.*

Term	Estimate	HC3 SE	95% CI	p	Exp(beta)
Intercept / reference level	-4.485	0.101	[-4.683, -4.287]	<0.001	0.011
Month: Feb vs Jan	0.059	0.104	[-0.146, 0.263]	0.574	1.06
Month: Mar vs Jan	-0.003	0.103	[-0.206, 0.200]	0.975	0.997
Month: Apr vs Jan	0.035	0.107	[-0.174, 0.244]	0.741	1.036
Month: May vs Jan	0.025	0.106	[-0.182, 0.232]	0.811	1.026
Month: Jun vs Jan	0.057	0.107	[-0.154, 0.267]	0.597	1.058
Month: Nov vs Jan	-0.158	0.163	[-0.478, 0.161]	0.332	0.854
Month: Dec vs Jan	0.014	0.105	[-0.193, 0.220]	0.897	1.014
Day of week: Tue vs Mon	0.107	0.107	[-0.103, 0.317]	0.317	1.113
Day of week: Wed vs Mon	0.095	0.107	[-0.115, 0.305]	0.375	1.1
Day of week: Thu vs Mon	0.083	0.107	[-0.127, 0.292]	0.439	1.086
Day of week: Fri vs Mon	0.064	0.107	[-0.146, 0.275]	0.549	1.067
Day of week: Sat vs Mon	-0.156	0.108	[-0.367, 0.055]	0.148	0.856
Day of week: Sun vs Mon	-0.282	0.109	[-0.495, -0.070]	0.009	0.754

Reference categories: January and Monday. ***Source:*** *own elaboration.*

Table 4B: *Complete HC3 coefficient table for Model B: log daily mean E ~ month + day of week + probe fixed effects.*

Term	Estimate	HC3 SE	95% CI	p	Exp(beta)
Intercept / reference level	-2.045	0.022	[-2.089, -2.001]	<0.001	0.129
Month: Feb vs Jan	0.062	0.016	[0.030, 0.094]	<0.001	1.064
Month: Mar vs Jan	0.001	0.018	[-0.035, 0.037]	0.972	1.001
Month: Apr vs Jan	0.039	0.018	[0.003, 0.075]	0.032	1.04
Month: May vs Jan	0.029	0.017	[-0.004, 0.062]	0.084	1.029
Month: Jun vs Jan	0.031	0.018	[-0.003, 0.066]	0.077	1.032
Month: Nov vs Jan	-0.26	0.046	[-0.351, -0.169]	<0.001	0.771
Month: Dec vs Jan	0.041	0.021	[-0.000, 0.081]	0.050	1.041
Day of week: Tue vs Mon	0.107	0.021	[0.066, 0.149]	<0.001	1.113
Day of week: Wed vs Mon	0.105	0.021	[0.064, 0.147]	<0.001	1.111
Day of week: Thu vs Mon	0.095	0.022	[0.052, 0.137]	<0.001	1.099
Day of week: Fri vs Mon	0.066	0.022	[0.023, 0.109]	0.003	1.068
Day of week: Sat vs Mon	-0.15	0.022	[-0.193, -0.107]	<0.001	0.861
Day of week: Sun vs Mon	-0.276	0.024	[-0.323, -0.230]	<0.001	0.759
Probe: Bogota_AEROPUERTO_GUAYMARAL vs Bogota_AEROCIVIL	-2.677	0.019	[-2.715, -2.640]	<0.001	0.069
Probe: Bogota_ANE vs Bogota_AEROCIVIL	-3.549	0.021	[-3.590, -3.508]	<0.001	0.029
Probe: Bogota_ANE_2 vs Bogota_AEROCIVIL	-0.999	0.014	[-1.026, -0.972]	<0.001	0.368
Probe: Bogota_BATALLON_BARAYA vs Bogota_AEROCIVIL	-2.465	0.016	[-2.497, -2.434]	<0.001	0.085
Probe: Bogota_BATALLON_USME vs Bogota_AEROCIVIL	-3.707	0.022	[-3.750, -3.665]	<0.001	0.025
Probe: Bogota_CAN_CGFM vs Bogota_AEROCIVIL	-2.505	0.016	[-2.537, -2.473]	<0.001	0.082
Probe: Bogota_MINTIC vs Bogota_AEROCIVIL	-2.09	0.02	[-2.129, -2.050]	<0.001	0.124
Probe: Bogota_TES_1 vs Bogota_AEROCIVIL	-4.048	0.03	[-4.106, -3.990]	<0.001	0.017

Reference categories: January, Monday, and Bogota_AEROCIVIL. ***Source:*** *own elaboration.*

After adjustment for probe, temporal effects became more stable and interpretable. Relative to January, February showed a 6.4% increase in daily mean exposure, April showed a 4.0% increase, and November was 22.9% lower. Relative to Monday, Tuesday through Friday were higher, while Saturday and Sunday were lower. These effects are meaningful, but their magnitude is much smaller than the site coefficients.

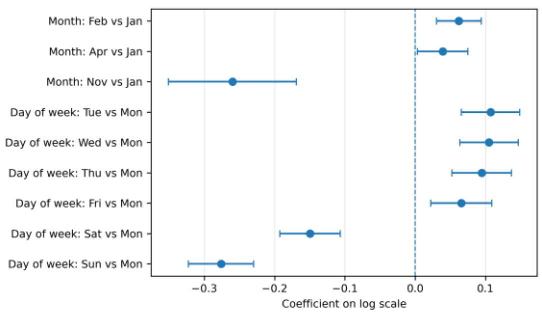

Fig. 4. *Selected temporal effects from the probe-adjusted model. Coefficients are shown on the log scale relative to January and Monday.* ***Source:*** *own elaboration.*

3.3. Regression diagnostics, p95 robustness, and mixed-effects robustness

The high adjusted R^2 of Model B required diagnostic verification. Table 5 shows that residuals were not normally distributed and that heteroskedasticity was present; therefore, HC3 robust standard errors were used for coefficient inference. The diagnostics also showed positive residual autocorrelation, with a pooled Durbin-Watson value of 0.598 and a median probe-level lag-1 residual autocorrelation of 0.641. This autocorrelation means that exact temporal p-values should be interpreted cautiously, especially for month effects. However, the influence diagnostics did not indicate that the model fit was being driven by a small number of leverage points: the maximum leverage was 0.0147, below the 2p/n threshold, and the maximum Cook's distance was 0.0278.

Table 5: *Regression diagnostics for Model B.*

Diagnostic	Result
Shapiro-Wilk residual normality	W = 0.926, p < 0.001
Jarque-Bera residual normality	JB = 3532.7, skew = -1.194, kurtosis = 9.041, p < 0.001
Breusch-Pagan heteroskedasticity	LM = 312.4, p < 0.001
Pooled Durbin-Watson	0.598
Median probe-level lag-1 residual ACF	0.641
Range of probe-level lag-1 residual ACF	0.222 to 0.936
Maximum leverage	0.0147
Leverage above 2p/n	0 observations (threshold = 0.0219)
Maximum Cook's distance	0.0278
Cook's distance above 4/n	98 observations (threshold = 0.0020)
Studentized residuals |r| > 3	23 of 2009 observations

The diagnostics qualify inference and support the use of robust and panel-aware checks. ***Source:*** *own elaboration.*

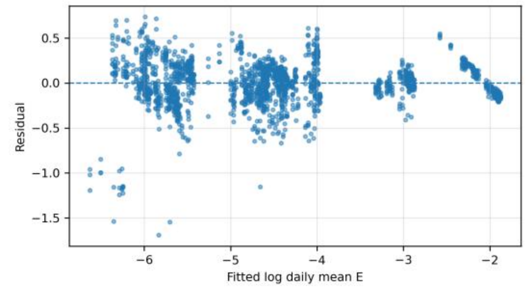

Fig. 5. *Residuals versus fitted values for Model B.* ***Source:*** *own elaboration.*

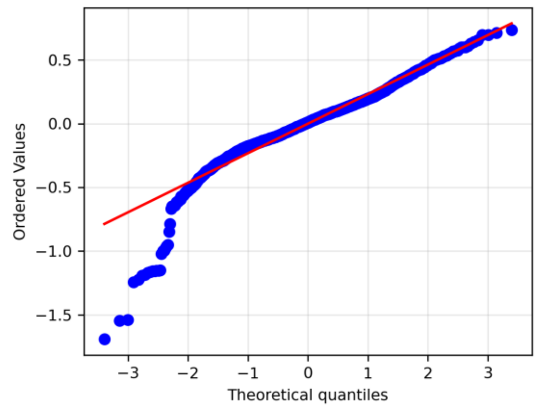

Fig. 6. *Q-Q plot of Model B residuals.* ***Source:*** *own elaboration.*

The p95 model directly addressed the reviewer's concern about excluding the upper-tail metric from inferential analysis. The p95 model achieved an adjusted R^2 of 0.951, and its coefficients retained the same qualitative structure as the mean model: upper-tail exposure was still dominated by persistent site differences, while weekday effects remained visible and weekends were lower. Selected p95 coefficients are shown in Table 6; the complete p95 coefficient table is exported by the revised R script.

Table 6: *Selected coefficients from the complementary p95 model.*

Term	Estimate	HC3 SE	95% CI	p	Exp(beta)
Month: Feb vs Jan	0.07	0.02	[0.030, 0.109]	<0.001	1.072

Month: Apr vs Jan	0.079	0.023	[0.034, 0.123]	<0.001	1.082
Month: Nov vs Jan	-0.219	0.043	[-0.302, -0.135]	<0.001	0.804
Day of week: Tue vs Mon	0.149	0.025	[0.099, 0.199]	<0.001	1.161
Day of week: Sun vs Mon	-0.346	0.029	[-0.402, -0.289]	<0.001	0.708
Probe: Bogota_ANE_2 vs Bogota_AEROCIVIL	-0.629	0.017	[-0.663, -0.595]	<0.001	0.533
Probe: Bogota_MINTIC vs Bogota_AEROCIVIL	-1.671	0.026	[-1.723, -1.620]	<0.001	0.188
Probe: Bogota_TES_1 vs Bogota_AEROCIVIL	-3.908	0.029	[-3.965, -3.851]	<0.001	0.02

Response variable: log daily p95 E. Reference categories: January, Monday, and Bogota_AEROCIVIL.
Source: *own elaboration.*

The random-intercept mixed model provided a second robustness check for the longitudinal structure. When probe was modeled as a random intercept instead of as fixed probe indicators, the marginal R^2 associated with temporal fixed effects alone was 0.016, while the conditional R^2 including the probe-level structure was 0.964. This result is consistent with Model B and confirms that the dominant structure in the Bogotá archive is the persistent difference between monitoring sites rather than month or weekday alone.

3.4. Technical interpretation of site and temporal effects

Bogota_AEROCIVIL was the highest-output site in both descriptive and adjusted analyses. Because the ANE release does not include source-resolved or frequency-selective metadata, this result should not be interpreted as a causal estimate of a specific transmitter or service. A technical, non-causal explanation is that the site may be located in a denser radio environment, potentially influenced by surrounding telecommunications infrastructure, aviation-related or institutional communications, rooftop or macrocell deployments, line-of-sight conditions, and local urban propagation features. Broadband monitors integrate all active services within their measurement band, so a persistent elevation at a fixed probe is technically plausible even when absolute levels remain far below public reference values.

The sign reversal for November is also explained by site composition. In the raw monthly profile, November appears elevated because the earliest part of the archive includes a strong contribution from higher-output probes, particularly Bogota_AEROCIVIL. Once the model holds the probe constant, November is no longer compared as a simple city-wide average; it is compared within the same site baseline. The adjusted November coefficient therefore becomes negative relative to January. This is not a contradiction but an example of confounding between calendar effects and monitoring-site composition.

The weekday pattern is more stable. Tuesday through Friday were higher than Monday, whereas Saturday and Sunday were lower in both mean and p95 specifications. From an engineering perspective, this supports the interpretation that recurring weekly changes in aggregate network activity modulate the measured field. Nevertheless, the much larger probe effects show that weekly modulation is secondary to persistent site conditions.

3.5. Engineering implications, limitations, and data governance

Restricting the analysis to Bogotá changes the practical meaning of the results. The model is not comparing heterogeneous cities; it is comparing multiple fixed monitors within one metropolitan radio environment. Site-specific baselines are therefore better suited than city-wide grand means for benchmarking normal conditions, communicating expected ranges at each probe, and identifying days that deserve follow-up.

High-output sites such as Bogota_AEROCIVIL and Bogota_ANE_2 are natural candidates for closer trend monitoring or targeted audits, not because they approach restrictive public limits, but because changes in the surrounding radio environment are more likely to become detectable there. Conversely, lower-output probes provide useful reference contexts for anomaly screening and public communication about how strongly exposure can vary across the same city while remaining low in absolute terms.

The inconsistency between the archived 28 V/m documentation and the current CSV fields Limite_Restrictivo and Porcentaje_Exposicion reinforces the importance of modeling the directly measured variable in V/m rather than relying on derived percentage fields. Public monitoring archives are analytically valuable only if their variable semantics are audited as carefully as the statistical procedure itself.

This study also has limitations. The released dataset does not provide source-resolved, frequency-selective, traffic, antenna, or meteorological metadata, so site effects should not be interpreted as causal estimates of specific transmitters or technologies. The release window covers eight months, which is sufficient for short-term structure but not for multi-year evolution. Daily aggregation suppresses intraday dynamics, and residual autocorrelation suggests that future work should extend the workflow toward hourly models, generalized least squares, autoregressive structures, change-point analysis, or frequency-resolved monitoring as richer releases become available, particularly under newer 5G deployment scenarios [24], [25].

4. CONCLUSIONS

This study reorganized the ANE open monitoring archive around a single metropolitan case: Bogotá. From 481,148 six-minute broadband measurements collected by nine fixed probes, the workflow constructed 2,009 near-complete probe-day records and used them to characterize exposure levels, compare temporal and site-adjusted models, evaluate diagnostics, and test p95 and mixed-effects robustness.

The descriptive results showed that field levels in Bogotá remained low in absolute terms. The highest observed six-minute value was 0.21011 V/m, still below 1% of the contextual 28 V/m public reference described in the archived documentation. At the same time, the city exhibited pronounced between-site heterogeneity, with Bogota_AEROCIVIL and Bogota_ANE_2 consistently occupying the upper end of the distribution.

The modeling results sharpened that interpretation. A temporal-only model explained almost none of the variation, whereas the probe-adjusted model explained most of it. Diagnostics showed heteroskedasticity, non-normality, and residual autocorrelation, but the high fit was not produced by high-leverage observations. The p95 model and the random-intercept mixed model supported the same conclusion: temporal variation exists, but persistent site-specific behavior is the dominant structure in the Bogotá archive.

The main contribution is therefore methodological and operational. Open continuous monitoring data can support interpretable site-aware analytics when preprocessing rules are explicit, variable semantics are audited, complete model outputs are reported, and upper-tail behavior is checked. For Bogotá, the results support probe-level baselines for benchmarking, anomaly screening, and public technical communication. The revised R workflow can be reused for future ANE releases or extended to richer monitoring contexts as additional metadata become available.

Author Contributions: Following the CRediT (Contributor Roles Taxonomy) framework, the contributions of each author were as follows: Conceptualization: O.B.-C., J.G.P.-H., and C.D.C.-A.; data curation: O.B.-C. and C.D.C.-A.; formal analysis: O.B.-C. and C.D.C.-A.; funding acquisition: none; investigation: O.B.-C., J.G.P.-H., and C.D.C.-A.; methodology: O.B.-C., J.G.P.-H., and C.D.C.-A.; project administration: O.B.-C., J.G.P.-H., and C.D.C.-A.; resources: O.B.-C.; software: O.B.-C., J.G.P.-H., and C.D.C.-A.; supervision: O.B.-C., J.G.P.-H., and C.D.C.-A.; validation: O.B.-C., J.G.P.-H., and C.D.C.-A.; visualization: O.B.-C.; writing—original draft: O.B.-C., J.G.P.-H., and C.D.C.-A.; writing—review and editing: O.B.-C., J.G.P.-H., and C.D.C.-A. All authors have read and approved the final version of the manuscript.

Funding: This research received no external funding.

Materials and Data Availability: The raw monitoring data are publicly available from the Colombian open data portal maintained by the Agencia Nacional del Espectro [5]. The revised Bogotá-specific R workflow generates the derived probe-day dataset, complete coefficient tables, diagnostics, figures, and reproducibility metadata accompanying this manuscript.

Acknowledgments: The authors acknowledge the Agencia Nacional del Espectro for publishing the continuous monitoring dataset used in this study.

Use of Generative AI: During revision of this manuscript, a generative AI assistant was used to support language editing, translation, document organization, and preparation of responses to reviewers. Numerical results were generated from the provided dataset through auditable code and were reviewed by the authors. The authors take full responsibility for the final content, interpretation, and conclusions of this publication.

REFERENCES

[1] World Health Organization, “Electromagnetic fields,” WHO Health Topics. [Online]. Available: https://www.who.int/health-topics/electromagnetic-fields (accessed Apr. 2025).

[2] World Health Organization, “Radiation: Electromagnetic fields,” WHO Questions and Answers. [Online]. Available: https://www.who.int/news-room/questions-and-answers/item/radiation-electromagnetic-fields (accessed Apr. 2025).

[3] International Telecommunication Union, “Recommendation ITU-T K.83: Monitoring of electromagnetic field levels,” ITU-T, Geneva, Switzerland, Aug. 2024. [Online]. Available: https://www.itu.int/rec/T-REC-K.83-202408-I

[4] Agencia Nacional del Espectro, “Resolución 774 de 2018 por la cual se establecen los límites de exposición de las personas a los campos electromagnéticos,” ANE, Bogotá, Colombia, 2018. [Online]. Available: https://www.ane.gov.co/Documentos%20compartidos/ArchivosDescargables/Normatividad/Radiaciones_no_ionizantes/Resol_774-2018.pdf

[5] Agencia Nacional del Espectro, “Mediciones de exposición a campos electromagnéticos del sistema de monitoreo de campos electromagnéticos: Documento soporte datos abiertos,” ANE, Bogotá, Colombia, 2020. [Online]. Available: https://www.ane.gov.co/Documentos%20compartidos/ArchivosDescargables/datos-abiertos/Documento%20Soporte%20Datos%20Abiertos.pdf

[6] International Commission on Non-Ionizing Radiation Protection, “Guidelines for limiting exposure to electromagnetic fields (100 kHz to 300 GHz),” Health Phys., vol. 118, no. 5, pp. 483–524, May 2020, doi: 10.1097/HP.0000000000001210.

[7] G. Dürrenberger, J. Fröhlich, M. Röösli, and M.-O. Mattsson, “EMF monitoring—concepts, activities, gaps and options,” Int. J. Environ. Res. Public Health, vol. 11, no. 9, pp. 9460–9479, Sep. 2014, doi: 10.3390/ijerph110909460.

[8] S. Sagar, S. Dongus, A. Schoeni, K. Roser, M. Eeftens, B. Struchen, M. Foerster, N. Meier, S. Adem, and M. Röösli, “Radiofrequency electromagnetic field exposure in everyday microenvironments in Europe: A systematic literature review,” J. Expo. Sci. Environ. Epidemiol., vol. 28, no. 2, pp. 147–160, Mar. 2018, doi: 10.1038/jes.2017.13.

[9] H. Jalilian, M. Eeftens, M. Ziaei, and M. Röösli, “Public exposure to radiofrequency electromagnetic fields in everyday microenvironments: An updated systematic review for Europe,” Environ. Res., vol. 176, art. no. 108517, Sep. 2019, doi: 10.1016/j.envres.2019.05.048.

[10] A. Manassas, A. Boursianis, T. Samaras, and J. N. Sahalos, “Continuous electromagnetic radiation monitoring in the environment: Analysis of the results in Greece,” Radiat. Prot. Dosimetry, vol. 151, no. 3, pp. 437–442, Sep. 2012, doi: 10.1093/rpd/ncs028.

[11] I. Karastergios, A. Gialofas, and E. Karabetsos, “National observatory of electromagnetic fields: National telemetric network for the measurement of high-frequency electromagnetic fields in Greece,” Radiat. Prot. Dosimetry, vol. 188, no. 4, pp. 413–423, Jul. 2020, doi: 10.1093/rpd/ncz301.

[12] A. Manassas, C. Apostolidis, S. Iakovidis, D. Babas, and T. Samaras, “A study of the long term changes in the electromagnetic environment using data from continuous monitoring sensors in Greece,” Sci. Rep., vol. 13, art. no. 13784, Aug. 2023, doi: 10.1038/s41598-023-41034-3.

[13] P. A. Valberg, T. E. van Deventer, and M. H. Repacholi, “Workgroup report: Base stations and wireless networks—radiofrequency (RF) exposures and health consequences,” Environ. Health Perspect., vol. 115, no. 3, pp. 416–424, Mar. 2007, doi: 10.1289/ehp.9633.

[14] P. Frei, E. Mohler, G. Neubauer, G. Theis, A. Bürgi, J. Fröhlich, C. Braun-Fahrländer, J. Bolte, M. Egger, and M. Röösli, “Temporal and spatial variability of personal exposure to radio frequency electromagnetic fields,” Environ. Res., vol. 109, no. 6, pp. 779–785, Aug. 2009, doi: 10.1016/j.envres.2009.04.015.

[15] W. Joseph et al., “Comparison of personal radio frequency electromagnetic field exposure in different urban areas across Europe,” Environ. Res., vol. 110, no. 7, pp. 658–663, Oct. 2010, doi: 10.1016/j.envres.2010.06.009.

[16] A. Bürgi, D. Scanferla, and H. Lehmann, “A model for radiofrequency electromagnetic field predictions at outdoor and indoor

locations in the context of epidemiological research," Bioelectromagnetics, vol. 31, no. 3, pp. 226–236, Apr. 2010, doi: 10.1002/bem.20552.

[17] S. Aerts et al., "Exposure assessment of mobile phone base station radiation in an outdoor environment using sequential surrogate modeling," Bioelectromagnetics, vol. 34, no. 4, pp. 300–311, May 2013, doi: 10.1002/bem.21764.

[18] J. Beekhuizen, R. Vermeulen, H. Kromhout, A. Bürgi, and A. Huss, "Geospatial modelling of electromagnetic fields from mobile phone base stations," Sci. Total Environ., vols. 445–446, pp. 202–209, Feb. 2013, doi: 10.1016/j.scitotenv.2012.12.020.

[19] D. Urbinello, W. Joseph, L. Verloock, L. Martens, and M. Röösli, "Temporal trends of radio-frequency electromagnetic field exposure in everyday environments across European cities," Environ. Res., vol. 134, pp. 134–142, Oct. 2014, doi: 10.1016/j.envres.2014.07.003.

[20] S. Aerts, W. Joseph, D. Deschrijver, L. Verloock, T. Dhaene, and L. Martens, "Assessment of long-term spatio-temporal radiofrequency electromagnetic field exposure," Environ. Res., vol. 161, pp. 136–143, Feb. 2018, doi: 10.1016/j.envres.2017.11.003.

[21] S. Sagar et al., "Comparison of radiofrequency electromagnetic field exposure levels in different everyday microenvironments in an international context," Environ. Int., vol. 114, pp. 297–306, May 2018, doi: 10.1016/j.envint.2018.02.036.

[22] R Core Team, "R: A Language and Environment for Statistical Computing," R Foundation for Statistical Computing, Vienna, Austria, 2024. [Online]. Available: https://www.R-project.org/.

[23] M. J. van Wyk, J. C. Visser, and C. W. le Roux, "Measurement of EMF exposure around small cell base station sites," Radiat. Prot. Dosimetry, vol. 184, no. 2, pp. 211–215, Aug. 2019, doi: 10.1093/rpd/ncy201.

[24] S. Aerts et al., "RF-EMF exposure near 5G NR small cells," Sensors, vol. 23, no. 6, art. no. 3145, Mar. 2023, doi: 10.3390/s23063145.

[25] S. Liu, K. Tobita, T. Onishi, M. Taki, and S. Watanabe, "Electromagnetic field exposure monitoring of commercial 28-GHz band 5G base stations in Tokyo, Japan," Bioelectromagnetics, vol. 45, no. 6, pp. 281–292, Sep. 2024, doi: 10.1002/bem.22505.

[26] J. C. Pinheiro and D. M. Bates, Mixed-Effects Models in S and S-PLUS. New York, NY, USA: Springer, 2000.

[27] J. M. Wooldridge, Econometric Analysis of Cross Section and Panel Data, 2nd ed. Cambridge, MA, USA: MIT Press, 2010.

[28] J. Fox and S. Weisberg, An R Companion to Applied Regression, 3rd ed. Thousand Oaks, CA, USA: Sage, 2019.